JOURNAL OF AGRICULTURAL AND FOOD CHEMISTRY
ARTICLE

J. Agric. Food Chem. 2011, 59, 727–732 727
DOI:10.1021/jf103441p

Thermodynamics and Structural Features of the Yeast *Saccharomyces cerevisiae* External Invertase Isoforms in Guanidinium-chloride Solutions

Uroš Andjelković[†] and Jurij Lah*[,‡]

[†]Institute for Chemistry, Technology and Metallurgy, Department of Chemistry, University of Belgrade, Studentski trg 12−16, 11000 Belgrade, Serbia, and [‡]Faculty of Chemistry and Chemical Technology, University of Ljubljana, Aškerčeva 5, 1000 Ljubljana, Slovenia

Recently, four external invertase isoforms (EINV1, EINV2, EINV3, and EINV4) have been isolated from *S. cerevisiae*. However, there is nothing known about their structural features and thermodynamics of unfolding. Since this information is essential for understanding their functioning at the molecular level as well as applicable in the food industry, we investigated guanidinium-chloride induced structural changes of the isoforms by CD and fluorescence spectroscopy. The resulting unfolding curves measured for each isoform at different temperatures were described simultaneously by a reversible two-state model to obtain the corresponding thermodynamic parameters. Here, we show that they are different for different isoforms and demonstrate that they correlate with the surface charge density of the native isoforms which follows the order EINV1 < EINV2 < EINV3 < EINV4. It appears that at physiological temperatures the thermodynamic stability of the isoforms follows the same order, while above 55 °C, the order is the opposite EINV1 > EINV2 > EINV3 ≈ EINV4. This suggests that increasing the efficiency of the food industry processes involving invertase would require the application of EINV3 and/or EINV4 at physiological temperatures and EINV1 at elevated temperatures.

KEYWORDS: Invertase; isoform; thermodynamics; unfolding; posttranslational modification; glycoprotein stability; *Saccharomyces cerevisiae*;

1. INTRODUCTION

Invertase (β-fructofuranosid fructohydrolase, EC 3.2.1.26) catalyzes the hydrolysis of sucrose into an equimolar mixture of glucose and fructose, known as invert sugar. Because of the higher sweetness, invert sugar is preferred over sucrose in the food industry (the same level of sweetness can be achieved with lower amount of sugar). It is preferred also due to lower crystallinity, ensuring that the products remain fresh and soft for a long period of time. Production of invert sugar by invertase has exclusive advantage over chemical catalysis because a colorless product is obtained in higher yield and without furfural (*1*). It is used for the prevention of crystalyzation in molasses storage tanks and for increasing the yield of production of ethanol from molasses (*2*). External invertase is a widely used model enzyme to study different immobilization matrixes for the food industry (*3*, *4*). Besides, sucrose invertase can degrade other substrates such as 1-kestose, raffinose, and stachyose.

Invertase has been found in different organisms. However, yeast *S. cerevisiae* is the main source of invertase in the food industry. *S. cerevisiae* synthesizes two forms of invertase with the same amino acid sequence: the external (glycosylated) and the internal (nonglycosylated) (*5*, *6*). The external invertase is of industrial importance due to the presence of a carbohydrate component, which increases its thermal stability (*7*), resistance against protease (*8*), and solubility (*9*), and makes the enzyme extremely stable at room temperature (*10*). External invertase is active as a homodimer, which may dissociate at denaturing conditions (*5*, *7*). There are 14 potential N- glycosylation sites in the invertase sequence of which 13 are wholly or partially glycosylated to give an average of 9−10 oligosaccharides per subunit (*11*, *12*). Approximately 50% of the external invertase mass is polymannan, and 3% is glucosamine (*13*). The polymannan component contains covalently bound phosphate groups (*15*).

S. cerevisiae synthesizes at least four isoforms of external invertase (EINV1−EINV4), which exhibit differences in pI, thermal stability, and chemical reactivity due to differences in posttranslational modifications (*14*).

Yeasts are important source of enzymes in the food industry. Yeasts are the cheapest and are easily handled eukaryotic systems. They are widely used as commercial systems for the expression of N-glycosylated proteins since prokaryotic systems (*E. coli*) cannot biosynthesize N-linked glycoproteins. Proteins naturally secreted by yeast or those expressed in yeast are characterized by a high degree and heterogeneity of glycosylation forms. In this light, the determination of thermodynamic stability of the external invertase isoforms is important for understanding the differences in structure and function caused by the differences

*Corresponding authors: Phone: +386-1-2419414. Fax: +386-1-2419425. E-mail: jurij.lah@fkkt.uni-lj.si.

Published on Web 12/23/2010

Table 1. Thermodynamic Parameters of Unfolding of External Invertase Isoforms in the Absence of the Denaturant at 25 °C[a]

isoform	ΔG^0 (kcal mol^{-1})	ΔH^0 (kcal mol^{-1})	ΔC^0_P (kcal mol^{-1} K^{-1})	$T\Delta S^0$ (kcal mol^{-1})	m (kcal mol^{-1} M^{-1})
EINV1	16.8 ± 0.3	16.4 ± 1.5	0.6 ± 0.2	- 0.4 ± 1.0	4.1 ± 0.2
EINV2	17.4 ± 0.3	25.0 ± 1.4	1.0 ± 0.2	7.5 ± 1.3	4.4 ± 0.2
EINV3	18.7 ± 0.4	27.8 ± 1.3	2.2 ± 0.2	9.1 ± 1.2	5.1 ± 0.2
EINV4	19.3 ± 0.6	32.4 ± 2.5	2.1 ± 0.3	13.0 ± 2.0	6.5 ± 0.4

[a] Parameters were obtained from global fitting the model function (eq 7) to GdmCl induced unfolding curves (**Figure 3**).

in glycosylation. Finally, such characterization may serve as a tool for the improvement of food industry processes by increasing enzyme stability and efficiency of immobilization.

The aim of this work was to study structural features of native and denatured states of external invertase isoforms in solution by CD and fluorescence spectroscopy. Moreover, a simultaneous (global) thermodynamic analysis of guanidinium chloride (GdmCl) induced unfolding of external invertase isoforms measured by fluorescence spectroscopy at various temperatures was performed to get a deeper insight into the unfolding mechanism. The obtained thermodynamic stability of the isoforms was dissected into enthalpic and entropic contributions and discussed in terms of differences in glycosylation and surface charge density of the isoforms. The importance of these findings for the application of invertase in the food industry has been considered.

2. MATERIALS AND METHODS

2.1. Materials. All chemicals were of analytical grade and obtained from Sigma Chemical Company (St. Louis, MO, USA), and guanidinium chloride was from Merck KGaA (Darmstadt, Germany). Lyophilized baker's yeast *Saccharomyces cerevisiae* external invertase (β-fructofuranosid fructohydrolase EC 3.2.1.26) grade VII was obtained from Sigma Chemical Co. (St. Louis, MO, USA).

2.2. Purification of the Four Isoformsof Yeast External Invertase . The lyophilizate (sample of total external invertase) was dissolved in 50 mM acetate buffer at pH 5.5 and loaded onto an ion-exchange column (HiTrap Q HP column (1 mL) (GE Healthcare)) equilibrated in the same buffer, using FPLC (ÄKTA purifier 100). Four isoforms (EINV1−EINV4) were separated applying step elution as described previously (*14*). Each peak was rechromatographed, on the same column. After the samples were desalted by gel filtration and concentrated by ultrafiltration, they were stored at −20 °C. Invertase concentration was obtained by measuring absorbance at 280 nm ($A_{280\ nm} = 2.25$ for 1 mg/mL invertase solution) (*16*).

2.3. CD Spectroscopy. CD spectroscopy measurements were performed with an AVIV Model 62A DS spectrometer (Aviv Associates, New Jersey, USA) with a computer controlled thermal control unit. Ellipticity in far UV range from 210 to 260 nm was measured in a 0.1 cm cuvette at 25 °C. The spectral bandwidth of 2 nm and an averaging time of 2 s were used for the collection of each data point.

2.4. Fluorescence Spectroscopy (FL). Fluorescence emission spectra were recorded using the Perkin-Elmer LS 50 luminescence spectrometer (Perkin-Elmer, USA), equipped with a thermally controlled cell holder and a cuvette of 1 cm path length. The emission spectra (290−420 nm) were recorded using excitation at 280 nm. GdmCl induced unfolding of external invertase isoforms was followed by measuring intrinsic emission fluorescence at 340 nm. Measurements were performed at several temperatures between 10 and 40 °C. GdmCl concentrations varied from 0 to 4 M in 50 mM acetate buffer at pH 5.0. The concentration of isoforms was 0.04 mg/mL.

2.5. Global Thermodynamic Analysis of Guanidinium Chloride Unfolding Curves. Several publications reveal that *S. cerevisiae* external invertase exists in buffer solutions in a dimeric (native) form, while in concentrated GdmCl solutions, it exists in a monomeric (denatured) form (see, for example, refs *5* and *7*). Therefore, one may describe the GdmCl induced unfolding of the external invertase isoforms as a reversible two-state transition between the native dimer (N_2) and the denatured monomer (D).

$$N_2 \overset{K_{T,d}}{\leftrightarrow} 2D \tag{1}$$

The apparent equilibrium constant $K_{T,d}$ is a function of temperature (T) and GdmCl concentration (d) and can be defined as follows (see, for example, refs *17*−*19*):

$$K_{T,d} = \frac{[D]^2}{[N_2]} = \frac{\alpha^2_{T,d}}{1-\alpha_{T,d}} 2c \tag{2}$$

where $\alpha_{T,d}$ is the fraction of the protein in the denatured state at given T and d $\alpha_{T,d} = [D]/c$, where c is the total protein (monomer) molar concentration), and $[N_2]$ and [D] are the molarities of N_2 and D, respectively. According to the model, $c = 2[N_2] + [D]$, and the fluorescence emission intensity ($FL_{\lambda,T,d}$) measured at a given excitation wavelength λ, T, and d can be expressed in terms of the corresponding contributions $FL_{N,\lambda,T,d}$ and $FL_{D,\lambda,T,d}$ that characterize pure states N_2 and D at a given concentration c as:

$$FL_{\lambda,T,d} = FL_{N,\lambda,T,d}(1-\alpha_{T,d}) + FL_{D,\lambda,T,d}\alpha_{T,d} \tag{3}$$

Since $FL_{N,\lambda,T,d}$ and $FL_{D,\lambda,T,d}$ can be estimated at any measured T as linear functions of d (pre- and posttransitional baselines; **Figure 2A**), the measured $\alpha_{T,d}$ can be expressed as follows (**Figure 2B**):

$$\alpha_{T,d} = \frac{FL_{\lambda,T,d} - FL_{N,\lambda,T,d}}{FL_{D,\lambda,T,d} - FL_{N,\lambda,T,d}} \tag{4}$$

However, $\alpha_{T,d}$ can be connected to the thermodynamics of unfolding through the two-state transition model (eq 1) according to which the linear dependence of the standard Gibbs free energy of unfolding ($\Delta G^0_{T,d}$) on d can be at any T expressed as:

$$\Delta G^o_{T,d} = \Delta G^o_T - m \cdot d \tag{5}$$

where m is an empirical parameter correlated strongly to the amount of protein surface area exposed to the solvent upon unfolding (*20*) and assumed to be temperature independent. ΔG^0_T is the standard Gibbs free energy of unfolding in the absence of denaturant ($d = 0$) that may be expressed in terms of the corresponding standard Gibbs free energy ($\Delta G_{T_0}{}^0$) and standard enthalpy of unfolding ($\Delta H_{T_0}{}^0$) at a reference temperature $T_0 = 25$ °C and standard heat capacity of unfolding (ΔC^0_P) (assumed to be temperature independent) through the Gibbs−Helmholtz relationship (integrated form):

$$\Delta G^o_T = T\left\{\frac{\Delta G^o_{T_o}}{T_o} + \Delta H^o_{T_o}\left[\frac{1}{T} - \frac{1}{T_o}\right] + \Delta C^o_P\left[1 - \frac{T_o}{T} - \ln\frac{T}{T_o}\right]\right\} \tag{6}$$

It follows from eqs 5 and 6 that the model (adjustable) parameters $\Delta G_{T_0}{}^0$, $\Delta H_{T_0}{}^0$, ΔC^0_P, and m define $\Delta G^0_{T,d}$ and also the corresponding $K_{T,d}$ ($K_{T,d} = \exp(-\Delta G^0_{T,d}/RT)$). Consequently, the model function for $\alpha_{T,d}$ is derived from eq 2 as follows:

$$\alpha_{T,d} = \sqrt{\left(\frac{K_{T,d}}{4c}\right)^2 + \frac{K_{T,d}}{2c}} - \frac{K_{T,d}}{4c} \tag{7}$$

It can be compared to $\alpha_{T,d}$ values determined experimentally from eq 4. The values of adjustable parameters (**Table 1**) were obtained using the nonlinear Levenberg−Marquardt regression procedure. Then, the best global fit (see, for example, refs *19* and *21*) values of $\Delta G_{T_0}{}^0$, $\Delta H_{T_0}{}^0$, and ΔC^0_P were used to estimate ΔG^0_T (from eq 6), ΔH^0_T from Kirchhoff's law,

$$\Delta H^o_T = \Delta H^o_{T_o} + \Delta C^o_P(T - T_o) \tag{8}$$

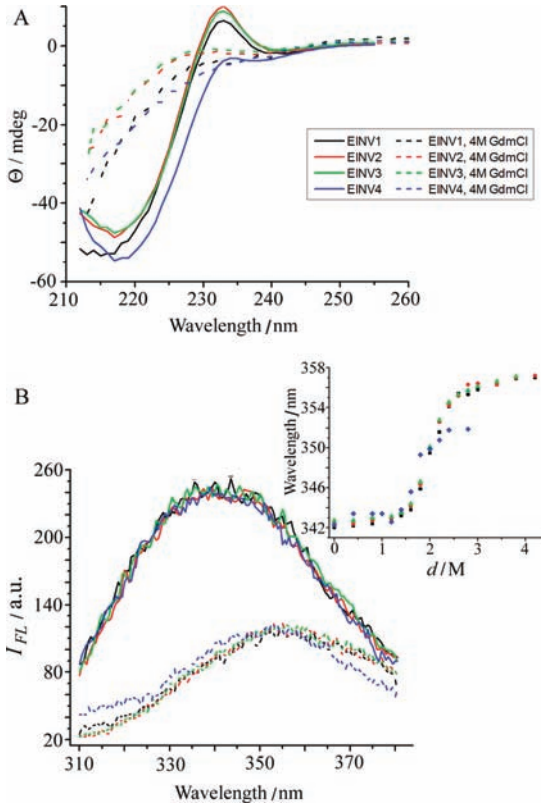

Figure 1. Structural features of external invertase isoforms in GdmCl aqueous solutions. (**A**) Comparison of the CD spectra of native (full line) and denatured with 4 M GdmCl (dotted line) external invertase isoforms (0.6 mg/mL) in 50 mM acetate buffer at pH 5.5 and 25 °C. (**B**) Comparison of intrinsic fluorescence emission spectra of native (full line) and denatured with 4 M GdmCl (dotted line) external invertase isoforms (0.04 mg/mL) in 50 mM acetate buffer at pH 5.5 and 25 °C. Inset: The corresponding wavelength shift of the emission maximum.

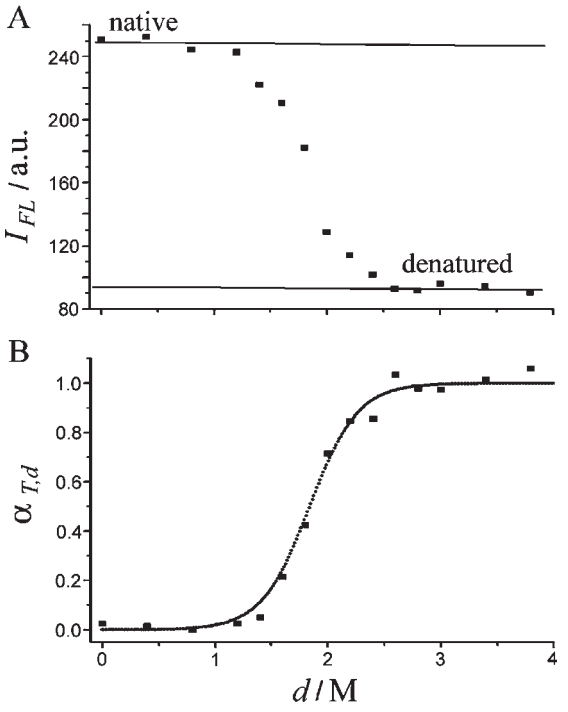

Figure 2. GdmCl induced unfolding of the external invertase isoform monitored by fluorescence spectroscopy. (**A**) Pre- and posttransitional baselines (full lines) define the intensity of fluorescence emission of the native and denatured states over the whole range of GdmCl concentrations. (**B**) The corresponding fraction of the isoform in the denatured state as a function of GdmCl concentration, *d*, obtained by eq 4. The figure shows an example of the EINV1 isoform unfolding at 25 °C (see **Figure 3**).

and the corresponding entropy contribution, $T\Delta S_T^0$, from the general relationship:

$$\Delta G_T^\circ = \Delta H_T^\circ - T\Delta S_T^\circ \quad (9)$$

The temperature dependences of ΔG_T^0, ΔH_T^0, and $T\Delta S_T^0$ are presented in **Figure 4**.

3. RESULTS AND DISCUSSION

3.1. Structural Features of External Invertase Isoforms in Solution. Observation of CD spectra of external invertase isoforms measured in buffer solution at pH 5.5 and 25 °C (**Figure 1A**) suggests that native isoforms contain relatively small amounts of α-helical structure and that the dominant secondary structural types are *β*-sheet and loop regions. The conformational features appear to be similar to those observed in 3D structures of the invertase of some other organisms (*22*). Moreover, the presence of loop regions, i.e., flexible regions, is consistent with the high degree of glycosylation (*23*). It can be seen from **Figure 1A** that in the native state EINV4 appears to be the only form that shows small but significant differences in secondary structure in comparison to the other three forms. However, changes of CD spectra accompanying GdmCl denaturation monitored around 220 nm suggest that about the same fraction of secondary structure is lost upon that process for all the isoforms. CD spectra of isoforms denatured with 4 M GdmCl show clear absence of native structure; however, they also suggest that isoforms retain a significant amount of the residual structure. Thus, the GdmCl denatured state of isoforms cannot be characterized as a completely unfolded state. This is consistent with previous results obtained for a sample of total external invertase (see section 2.2) (*24*).

Changes of the tryptophan residue environment upon the unfolding of external invertase isoforms in GdmCl solutions were monitored by fluorescence spectroscopy (**Figure 1B**). Fluorescence spectra of all four isoforms in the native state are identical, indicating that differences between isoforms do not have an impact on the environment of tryptophan residues. Unfolding is accompanied by lowering the fluorescence emission intensities and by red-shift of the emission maxima from 342 nm to wavelengths≥352 nm (**Figure 1B**, inset). Such changes are characteristic of the exposure of tryptophan residues to more polar (water−GdmCl) environments. In the denatured state of EINV4 (red shift ≈10 nm), tryptophan residues appear to be less exposed to the polar environment than in the denatured states of the other forms (red shift ≈15 nm). Together with the results of CD spectroscopy, this finding suggests that differences in glycosylation are responsible for small but significant differences in the secondary and tertiary structure of EINV4 in comparison to that of the other forms.

3.2. Thermodynamics of GdmCl Induced Unfolding. Thermally induced unfolding of yeast external invertase is an irreversible process accompanied by aggregation without precipitation (*25*). Therefore, thermodynamic parameters of unfolding cannot be obtained by an analysis of thermal unfolding curves. For this reason, we investigated the thermodynamics of external invertase isoforms unfolding by monitoring their reversible denaturation induced by GdmCl. Reversibility of denaturation transition was checked by the dilution of solutions of denatured isoforms with the corresponding buffer to obtain solutions in which the isoforms should exist in the native form. The extent of reversibility estimated by measuring fluorescence spectra before

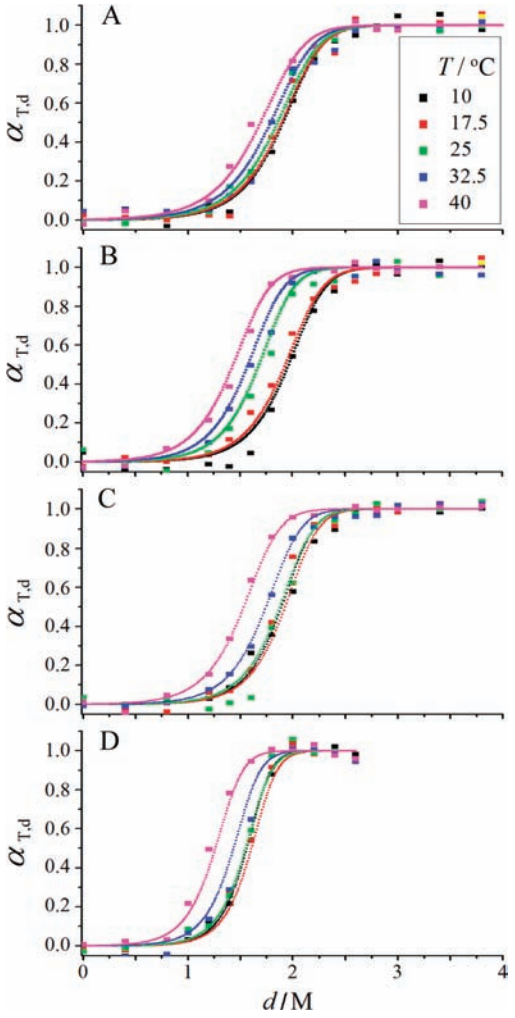

Figure 3. Global model analysis of GdmCl induced denaturation profiles. Fraction of the isoforms in the denatured state presented as a function of GdmCl concentration (see **Figure 2**, eq 4) expressed for the isoforms EINV1 (**A**), EINV2 (**B**), EINV3 (**C**), and EINV4 (**D**). Lines represent the best global fits of the model function (eq 7) to the experimental data points.

and 48 h after the dilution was more than 70%, which is in accordance with previous denaturation studies (*5*, *10*). GdmCl induced unfolding curves were obtained by monitoring changes in intrinsic emission fluorescence intensity at 340 nm and temperature T (**Figure 2A**), which were transferred into the dependence of the fraction of isoform in the denatured state, $\alpha_{T,d}$, on GdmCl concentration, d (eq 4; **Figure 2B**). Global fitting of the model function (eqs 5−7) to the unfolding curves of external invertase isoforms results in good agreement between the proposed reversible two-state model function and sets of unfolding curves measured at different temperatures (**Figure 3**). Here, it should be mentioned that an advantage of global fitting in comparison to step-by-step analysis of individual curves is that it uses fewer model parameters per given set of experimental data (*19*). Therefore and due to the observed good quality of the global fit, one may consider the obtained thermodynamic parameters as reliable and physically sound.

The thermodynamic profiles of unfolding of external invertase isoforms estimated from the best fit parameters (**Table 1**) are presented in **Figure 4**. Folding of the external invertase isoforms in the standard state at physiological temperature is an enthalpy driven process accompanied by a negative heat capacity change. This is a common feature of globular proteins (*26*). Thermodynamic

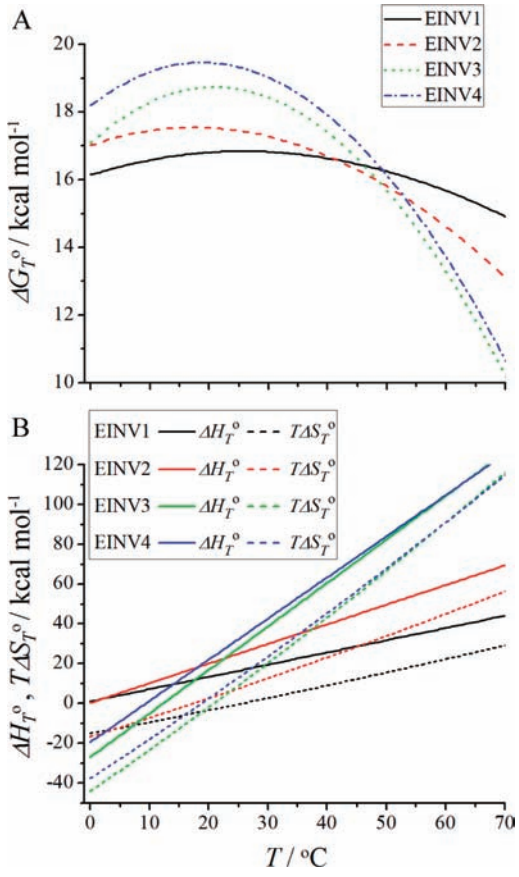

Figure 4. Thermodynamic profiles of EINV1 (black), EINV2 (red), EINV3 (green), and EINV4 (blue) unfolding. Standard Gibbs free energy, ΔG_T^0 (**A**), standard enthalpy, ΔH_T^0, and the corresponding entropy contribution, $T\Delta S_T^0$ (**B**) in the absence of GdmCl as a function of temperature (T) were estimated from the best fit parameters (**Table 1**) by using eqs 6, 8, and 9.

stabilities ΔG_T^0 of all four isoforms exhibit well-defined maxima between T values ~10 and 25 °C (**Figure 4A**). Isoform EINV4 exhibits the largest free energy difference between the unfolded and folded state, i.e., highest stability (**Figure 4A**), at physiological temperatures, followed by isoforms EINV3, EINV2, and EINV1 in descending order. In contrast, at temperatures higher than 55 °C the stability follows the order EINV1 > EINV2 > EINV3 ≈ EINV4. In addition, the obtained enthalpy and heat capacity of denaturation can be compared to the corresponding averages over a large set of proteins (*27*). The comparison shows that both measured quantities for all isoforms are significantly lower than the corresponding values expected for the protein of the same size. Thus, it may be concluded that the degree of unfolding of the isoforms in concentrated GdmCl solutions is significantly lower than the degree of unfolding seen in an average protein of the Robertson and Murphy data set. This is in accordance with results of CD spectroscopy showing that isoforms in the GdmCl denatured state retain a significant amount of the residual structure.

3.3. Thermodynamic Parameters of Unfolding Correlate with Surface Charge Density of the Native Isoforms. Several factors connected with glycosylation may influence biophysical characteristics of the protein: size of glycan, its flexibility and structure, the location and chemical surroundings of the glycosylation sites, the number of occupied glycosylation sites (*23*), and the presence of the covalently bound negatively charged groups to the glycan part (phosphate groups are attached to mannose units at the protein surface).

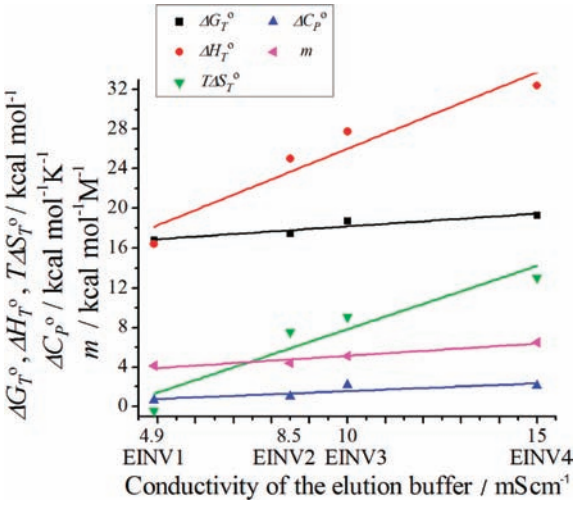

Figure 5. Thermodynamic parameters of external invertase isoforms at 25 °C as a function of the elution buffer (50 mM acetate buffer pH 5.5) conductivity (adjusted with NaCl) used for the elution of isoforms from the ion-exchange (QAE-Sephadex) column.

In this context, it has been shown recently (*14*) that the native isoforms exhibit differences in binding to the ion-exchange column. Binding affinity of the isoforms for the positively charged ion-exchange column and consequently the conductivity (ionic strength) of the buffer required for their effective elution follows the order EINV4 > EINV3 > EINV2 > EINV1 (**Figure 5**). This suggests that EINV4 has the highest negative surface charge density followed by isoforms EINV3, EINV2, and EINV1 in descending order. Since the protein part, i.e., number of amino acid residues, for all four isoforms is the same (*14*), it may be concluded that differences in surface charge density result from differences in posttranslational modifications. Moreover, the molecular weight of isoforms in SDS−PAGE has been shown to be identical, indicating that differences in their properties do not originate from different amounts of the carbohydrate component.

In this work, we have shown that all thermodynamic parameters of unfolding correlate with surface charge density of the native isoforms (**Figure 5**). However, since the influence of interactions of surface charges with other atomic groups, molecules, or ions to the thermodynamic characteristics of the protein native and denatured states is not well understood (*29*, *28*), it is not possible to give a reliable answer as to why such a correlation exists. This correlation supports a general finding that surface electrostatics is important for protein stability (*30*). It should be mentioned that differences in hydration of the native isoforms definitely contribute to the observed differences in all thermodynamic characteristics. The thermodynamic quantity that is closely related to the changes in hydration upon unfolding is ΔC^0_P. If we assume that the thermodynamics of hydration of all isoforms in the denatured state is about the same, the differences in ΔC^0_P could be attributed to the lower heat capacity of the native forms with higher surface charge density. Namely, according to the statistical thermodynamic theory, heat capacity is related to energy fluctuations. In this context, differences in heat capacities of the native forms may be explained by stronger association of water with surfaces characterized by higher charge densities; stronger association of the water molecules aggravates their fluctuations between the energy states (*30*).

In addition, the observed correlation of thermodynamic parameters of unfolding with the surface charge density of the native isoforms (**Figure 5**) may represent useful practical information for improving food industry processes. Namely, the order of thermodynamic stabilities of external invertase isoforms (**Figure 4A**) suggests that at physiological temperatures isoforms that are strongly bound to the ion-exchange column (EINV3 and EINV4) should be applied, but at elevated temperatures above 55 °C, the isoform EINV1 should be applied in order to increase the efficiency of food industry processes. Here, it should be pointed out that higher thermodynamic stability can certainly be very beneficial for industrial uses; however, other factors such as the enzyme's catalytic properties and resistance to chemical modifications are also important. In this light, we would like to mention that the observed highest thermodynamic stability of the isoform EINV1, at elevated temperatures, is in agreement with our previous findings that EINV1 exhibits the highest enzymatic stability at elevated temperatures (*14*). Moreover, it has been demonstrated (*14*) that the chemical reactivity of the invertase isoforms toward Eupergit C is in direct correlation with surface charge density.

Taken together, we show here for the first time that external invertase isoforms exhibit similar structural features in solution but significantly different thermodynamics of unfolding. We believe that the results contribute to the general understanding of the stability of external invertase. Since an understanding of factors that influence the stability of glycoproteins may enable the selection and design of enzymes with improved properties for efficient application, our approach may also be of practical importance.

LITERATURE CITED

(1) Bhatti, H. N.; Asgher, M.; Abbas, A.; Nawaz, R.; Sheikh, M. A. Studies on kinetics and thermostability of a novel acid invertase from *Fusarium solani*. *J. Agric. Food Chem.* **2006**, *54*, 4617−4623.

(2) Doelle, M. B.; Doelle, H. W. Ethanol production from sugar cane syrup using *Zymomonas mobilis*. *J. Biotechnol.* **1989**, *11*, 25−36.

(3) Kotwal, S. M.; Shankar, V. Immobilized invertase. *Biotechnol. Adv.* **2009**, *27*, 311−322.

(4) Vujčić, Z.; Milovanović, A.; Božić, N.; Dojnov, B.; Vujčić, M.; Andjelković, U.; Lončar, N. Immobilization of cell wall invertase modified with glutaraldehyde for continuous production of invert sugar. *J. Agric. Food Chem.* **2010**, *58*, 11896−11900.

(5) Kern, G.; Kern, D.; Jaenicke, R.; Seckler, R. Kinetics of folding and association of differently glycosylated variants of invertase from *Saccharomyces cerevisiae*. *Protein Sci.* **1993**, *2*, 1862−1868.

(6) Williams, R. S.; Trumbly, R. J.; MacColl, R.; Trimble, R. B.; Maley, F. Comparative properties of amplified external and internal invertase from the yeast SUC2 gene. *J. Biol. Chem.* **1985**, *260*, 13334−13341.

(7) Kern, G.; Schulke, N.; Schmid, F. X.; Jaenicke, R. Stability, quaternary structure, and folding of internal, external, and core-glycosylated invertase from yeast. *Protein Sci.* **1992**, *1*, 120−131.

(8) Chu, F. K.; Maley, F. The effect of glucose on the synthesis and glycosylation of the polypeptide moiety of yeast external invertase. *J. Biol. Chem.* **1980**, *255*, 6392−6397.

(9) Gascon, S.; Neumann, N. P.; Lampen, J. O. Comparative study of the properties of the purified internal and external invertases from yeast. *J. Biol. Chem.* **1968**, *243*, 1573−1577.

(10) Chu, F. K.; Trimble, R. B.; Maley, F. The effect of carbohydrate depletion on the properties of yeast external invertase. *J. Biol. Chem.* **1978**, *253*, 8691−8693.

(11) Ziegler, F. D.; Maley, F.; Trimble, R. B. Characterization of the glycosylation sites in yeast external invertase, II. *J. Biol. Chem.* **1988**, *263*, 6986−6992.

(12) Zeng, C.; Biemann, K. Determination of N-linked glycosylation of yeast external invertase by matrix-assisted laser desorption/ionization time-of-flight mass spectrometry. *J. Mass Spec.* **1999**, *34*, 311−329.

(13) Neumann, N. P.; Lampen, J. O. Purification and properties of yeast invertase. *Biochemistry* **1967**, *6*, 468−475.

(14) Andjelković, U.; Pićurić, S.; Vujčić, Z. Purification and characterisation of *Saccharomyces cerevisiae* external invertase isoforms. *Food Chem*. **2010**, *120*, 799−804.
(15) Trimble, R. B.; Maley, F.; Chu, F. K. Glycoprotein biosynthesis in yeast. *J. Biol. Chem*. **1983**, *258*, 2562−2567.
(16) Trimble, R. B.; Maley, F. Subunit structure of external invertase from *Saccharomyces cerevisiae*. *J. Biol. Chem*. **1977**, *252*, 4409−4412.
(17) Lah, J.; Prislan, I.; Kržan, B.; Salobir, M.; Francky, A.; Vesnaver, G. Erythropoietin unfolding: thermodynamic and its correlation with structural features. *Biochemistry* **2005**, *44*, 13883−13892.
(18) Šimić, M.; De Jonge, N.; Loris, R.; Vesnaver, G.; Lah, J. Driving force of gyrase recognition by the addiction toxin CcdB. *J. Biol. Chem*. **2009**, *248*, 20002−20010.
(19) Drobnak, I.; Vesnaver, G.; Lah, J. Model-based thermodynamic analysis of reversible unfolding processes. *J. Phys. Chem. B* **2010**, *114*, 8713−8722.
(20) Myers, J. K.; Pace, N. C.; Scholtz, M. J. Denaturant m values and heat capacity changes: relation to changes in accessible surface areas of protein unfolding. *Protein Sci*. **1995**, *4*, 2138−2148.
(21) Šimić, M.; Vesnaver, G.; Lah, J. Thermodynamic stability of the dimeric toxin CcdB. *Acta Chim. Slov*. **2009**, *56*, 139−144.
(22) Lammens, W.; Le Roy, K.; Van Laere, A.; Rabijns, A.; Van den Ende, W. Crystal structures of *Arbidopsis thaliana* cell-wall invertase mutants in complex with sucrose. *J. Mol. Biol*. **2008**, *377*, 378−385.
(23) Shental-Bechor, D.; Levy, Y. Folding of glycoproteins: toward understanding the biophysics of the glycosylation code. *Curr. Opin. Struct. Biol*. **2009**, *19*, 524−533.
(24) Sen, L.; Hai-Peng, Y.; Hai-Meng, Z. Inactivation and conformational changes of yeast invertase during unfolding in urea and guanidinium chloride solutions. *J. Pept. Res*. **1998**, *51*, 45−48.
(25) Schulke, N.; Schmid, F. X. The stability of yeast invertase is not significantly influenced by glycosylation. *J. Biol. Chem*. **1988**, *263*, 8827−8831.
(26) Makhatadze, G. I.; Privalov, P. L. Energetics of protein structure. *Adv. Protein Chem*. **1995**, *47*, 307−425.
(27) Robertson, A. D.; Murphy, K. P. Protein structure and the energetics of protein stability. *Chem. Rev*. **1997**, *97*, 1251−1267.
(28) Bončina, M.; Lah, J.; Reščič, J.; Vlachy, V. Thermodynamics of the lysozyme-salt interaction from calorimetric titrations. *J. Phys. Chem. B* **2010**, *114*, 4313−4319.
(29) Strickler, S. S.; Gribenko, Alexey V.; Gribenko, Alexander V.; Keiffer, T. R.; Tomlinson, J.; Reihle, T.; Loladze, V. V.; Makhatadze, G. I. Protein stability and surface electrostatics: a charged relationship. *Biochemistry* **2006**, *45*, 2761−2766.
(30) Sharp, K. A.; Madan, B. Hydrophobic effect, water structure, and heat capacity changes. *J. Phys. Chem. B* **1997**, *101*, 4343−4348.

Received for review September 7, 2010. Revised manuscript received November 23, 2010. Accepted November 28, 2010. U.A. acknowledges a grant from University of Ljubljana. This work was supported by the Slovenian Research Agency through Grant No. P1-0201 and by the Serbian Ministry of Science and Technological Development, Grant No. 142026B.